

University of Groningen

Spin transport in graphene - hexagonal boron nitride van der Waals heterostructures

Gurram, Mallikarjuna

IMPORTANT NOTE: You are advised to consult the publisher's version (publisher's PDF) if you wish to cite from it. Please check the document version below.

Document Version

Publisher's PDF, also known as Version of record

Publication date:

2018

[Link to publication in University of Groningen/UMCG research database](#)

Citation for published version (APA):

Gurram, M. (2018). *Spin transport in graphene - hexagonal boron nitride van der Waals heterostructures*. [Thesis fully internal (DIV), University of Groningen]. University of Groningen.

Copyright

Other than for strictly personal use, it is not permitted to download or to forward/distribute the text or part of it without the consent of the author(s) and/or copyright holder(s), unless the work is under an open content license (like Creative Commons).

The publication may also be distributed here under the terms of Article 25fa of the Dutch Copyright Act, indicated by the "Taverne" license. More information can be found on the University of Groningen website: <https://www.rug.nl/library/open-access/self-archiving-pure/taverne-amendment>.

Take-down policy

If you believe that this document breaches copyright please contact us providing details, and we will remove access to the work immediately and investigate your claim.

Downloaded from the University of Groningen/UMCG research database (Pure): <http://www.rug.nl/research/portal>. For technical reasons the number of authors shown on this cover page is limited to 10 maximum.

Abstract

In this chapter I describe the experimental techniques utilized for the work presented in this thesis. First, the mechanical exfoliation technique for finding individual flakes of graphene and hBN is described followed by the pick-up and transfer technique for making graphene-hBN van der Waals heterostructures. For the transfer of CVD grown hBN, the PMMA assisted transfer method is described. In the end, the measurement setup for the electrical characterization of the devices and various measurement geometries for the device characterization are also described.

4.1 Mechanical Exfoliation

Several attempts were made to obtain the thinnest form of the layered materials by mechanical exfoliation. Thin layers of highly oriented pyrolytic graphite (HOPG) down to 200 nm were obtained by controlled manipulation of graphite islands using an AFM tip either on HOPG or as-transferred on any flat substrate [1]. Later, this method was improved by picking up the HOPG islands using a tip-less AFM cantilever followed by stamping the island on a SiO₂ substrate in a tapping mode which resulted in cleaving the slabs of a graphite with minimum thickness 10 nm on the substrate [2].

While these nanofabrication techniques were good to obtain the thin graphite films, it was only the simplest method developed by the group of Andre Geim in 2004 resulted in obtaining a single layer of graphite, graphene [3]. This approach utilizes a household cellophane tape to peel off the layers from HOPG which successively is pressed down against a SiO₂/Si substrate to transfer the flakes. When the tape is taken away, van der Waals attraction forces between the graphite on the tape and the substrate leaves thinnest flakes down to monolayer on the substrate. A remarkable thing about their discovery is the identification of a monolayer graphene flake which is transparent and difficult to catch with naked eye due to its very small optical absorption [4, 5] of $\approx 2.3\%$. The group of Andre Geim utilized the interference effect of specially chosen 300 nm thick SiO₂ on Si substrate in order to increase the optical contrast of graphene flakes on the substrate [6].

The exfoliation approach was extended to other materials for the first time by Novoselov et al. [7] who reported the isolation of single layers of various 2D materials with high crystalline quality and macroscopic quantity, and stated the possibility of finding thin layers of hBN. Later it was Pacile et al. [8] who first reported the isolation of hBN flakes on a SiO_2/Si substrate using the exfoliation method.

4.2 Device preparation

In this section, I describe the steps involved in the preparation of a graphene-hBN heterostructure device for spin transport studies. Briefly, the device preparation starts with the mechanical exfoliation of graphene and hBN flakes followed by stacking them using the pick up and transfer technique. Then we use electron beam lithography for defining the electrodes pattern followed by deposition of the ferromagnetic electrodes before loading the device in the measurement setup for device characterization.

4.2.1 Exfoliation

1. One needs a clean substrate to exfoliate flakes of graphene and hBN. We use commercially available SiO_2/Si substrates (90 nm or 300 nm thick SiO_2 on top of 500 μm Si. Si is p-doped with resistivity 0.0001-0.0005 $\Omega\text{-cm}$). As obtained SiO_2/Si wafers were cut with a diamond scribe to a desired size ~ 20 mm x 10 mm and cleaned with the ultrasonication treatment; 2 minutes in acetone then 2 minutes in isopropyl alcohol (IPA), followed by blow dry with N_2 gas. Finally the substrate is furnace annealed at 180 $^\circ\text{C}$ for 10 minutes in order to remove organic residues and moisture.
2. We use HOPG (ZYA grade, PSI supplies) source for graphene flakes. A thick layer of graphite is peeled off from a HOPG source using an adhesive tape (Scotch tape). Another tape is used to peel off graphite from the first tape to thin down the graphite. It is repeated with two to three new tapes until the graphite on the last tape is thinned down to an optimum thickness.
3. The final tape with the optimum thickness of graphite is then pressed on top of a pre-cleaned SiO_2/Si substrate. A care should be taken for a uniform adhesion and removal of any air bubbles by gently pressing from the top using a rubber eraser or thumb. When the tape is peeled off from the substrate, we can observe the thick layers of graphite deposited on the SiO_2 substrate even with the naked eye.
4. Boron nitride flakes are exfoliated onto a different SiO_2/Si substrate from the small hBN crystals (~ 1 mm, supplier: HQ Graphene). The optical contrast of SiO_2 substrate allows the easy identification of hBN down to monolayers [9]. In

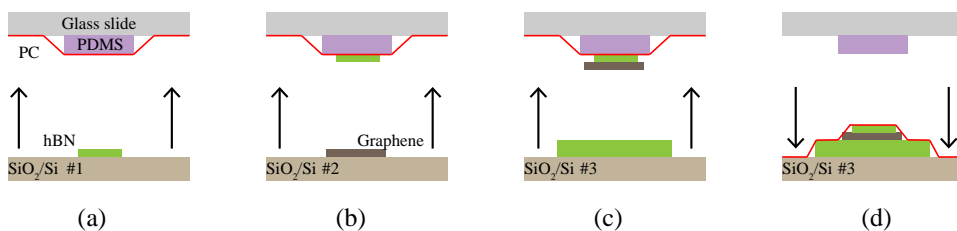


Figure 4.1: The pickup and transfer method for preparing hBN/graphene/hBN van der Waals heterostructures.

order to achieve an enhanced optical contrast and to easily identify the thinnest hBN flakes using the optical microscope, we use 90 nm thick SiO₂ [10].

5. The substrate with the exfoliated flakes is then scanned with an optical microscope to search for monolayer graphene or desired thickness of hBN (1-3 layers). Different thicknesses of flakes are identified from the optical contrast due to the interference effect with the underlying substrate. The optical contrast varies with the number of layers of flakes(1,2,3,...), material-type of flakes(graphene, hBN,...), type of substrate(SiO₂, hBN, PDMS,...), thickness of the substrate(300nm-SiO₂, 90nm-SiO₂, 10nm-hBN, 100 μ m PDMS,...), intensity and wavelength of the light used. Therefore, in the beginning of scanning, we first find a region with multilayer flakes and find the optical contrast for each layer which can be used as a reference for identifying the thickness of flakes that will be identified at the later stages of scanning.
6. Besides the optical contrast analysis, the flake thickness can also be obtained with an atomic force microscopy (AFM). However, the measured values are subject to the roughness of the substrate, and the glue residues from the scotch tape exfoliation. The measured thickness of monolayers of graphene and hBN using AFM vary 0.4-0.7 nm. An accurate determination of number of layers of flakes can be done via the Raman spectroscopy [11].

Once the flakes are identified and the thicknesses are determined, we proceed to prepare graphene-hBN heterostructures.

4.2.2 Pickup and transfer technique

The first transfer technique reported by Dean et al. [12] revolutionized the fabrication of vdW heterostructure devices. Thereafter many techniques were developed to make the process relatively easy and impurity free.

A fully encapsulated hBN/graphene/hBN heterostructure is prepared via the following dry pickup transfer method which was developed in our group [13].

1. We start with the preparation of a poly-bisphenol-A-carbonate (PC) solution by dissolving 6 wt.% of PC crystals in a chloroform solvent. We then prepare a thin film of PC on a glass slide. First, using a pipette, the PC solution is dropped on top of a glass slide on top of which another glass slide is pressed against to make a uniform spread of the PC solution. By quickly separating the glass slides, the evaporation of chloroform gives a thin layer of PC on both glass slides.
2. Next, a small opening of size $\approx 4 \times 4 \text{ mm}^2$ is cut out from a scotch tape using which some portion of the PC layer from the previously prepared glass slide is taken.
3. Now, we prepare another glass slide is prepared with a polydimethylsiloxane (PDMS) stamp sized $\approx 4 \times 4 \times 1 \text{ mm}^3$ and a scotch tape with PC layer is transferred on top. The whole set, consisting of the glass-slide/PDMS/PC, called mask, is used for picking up the pre-exfoliated graphene and hBN flakes subsequently.
4. The mask is then mounted on a mask aligner set up with the PC layer facing down. The substrates with the flakes to be picked up are fixed on a chuck of the mask aligner. Optical microscope is used for aligning the clean region of the mask with the desired flake to be picked up.
5. The chuck with the substrate can be manually brought close to the mask until the SiO_2 substrate is touching the PC. As soon as the flake is in a contact with the PC, we stop lifting the chuck and start heating it up to $\approx 60 \text{ }^\circ\text{C}$. As the SiO_2 substrate heats up, PC in contact will continue to expand and cover the flake. When the flake is completely covered by the PC, we switch off the heater to cool down the PC. As a result, PC will contract to its original shape while picking up the flake from SiO_2 substrate. In principle, the above procedure can be subsequently repeated to pick up multiple flakes.
6. In order to prepare the fully hBN encapsulaed devices in this thesis, we first picked up the hBN tunnel barrier (mono or bi or tri-layer of hBN)[Fig. 4.1(a)].
7. A single layer graphene (Gr) flake, exfoliated onto a different SiO_2/Si substrate is aligned with respect to the already picked up hBN tunnel barrier flake in the mask aligner[Fig. 4.1(b)]. When the graphene flake is brought in contact with the hBN-barrier flake on the PC film, it is picked up by the hBN-barrier flake due to van der Waals interactions between the flakes.
8. In the last step, the PC/hBN-barrier/Gr assembly is aligned with a thick-hBN flake on top of another SiO_2/Si substrate[Fig. 4.1(c)] and brought in a contact with the flake. The whole assembly is heated up to $\sim 150 \text{ }^\circ\text{C}$ and the PC film with the hBN-barrier/Gr is released onto the thick-hBN flake[Fig. 4.1(d)].

9. The PC film is then dissolved by submerging the stack in a chloroform solution for three hours at room temperature.
10. After the PC removal, the stack is annealed at 350 °C for 5 hours in Ar/H₂ environment for removing the polymer residues.

4.2.3 CVD-hBN transfer

For large scale applications, incorporating the chemical vapour deposition (CVD) grown materials is important. In order to explore this possibility, we also used CVD grown hBN tunnel barriers. Transfer of exfoliated-hBN tunnel barriers is done via pickup and transfer method as described above. For the transfer of CVD-hBN, we adopt a PMMA-assisted transfer (also called as wet-transfer) method [14] which has been widely used at the lab and industrial scale. The procedure for transferring CVD-hBN involves the following steps. We used CVD-hBN from two sources: commercially available from Graphene Supermarket Inc. and in-house grown by our collaborators [15] at Peking University, Beijing, China. The transfer of CVD-hBN is done in collaboration with the group of Prof. Christian Schönenberger at the University of Basel, Switzerland.

1. As obtained source of CVD-hBN comes with a monolayer grown on both sides of a copper (Cu) foil. We spin coat a PMMA (4%, of 950K average molecular weight dissolved in Anisole, 4000 rpm) layer on one side of the Cu foil to protect the CVD-hBN layer.
2. The spin coated film is annealed on hot plate at 180 °C for 2 minutes to remove the solvent in the spin coated PMMA.
3. The sacrificial CVD-hBN on the other side is removed using the physical dry etching (reactive ion etching with O₂ plasma, at 10 SCCM, 40 W, 45 sec).
4. Then the copper is removed using the chemical wet etching by floating the structure PMMA/CVD-hBN/Cu in a contact with an ammonium persulfate (NH₄)₂S₂O₄ etchant solution (87.6 mMol/L in DI water) for 12 hours.
5. While the PMMA/CVD-hBN is still floating, we replace the etchant with deionized (DI) water 3 to 4 times using a pipette. This will clean the contact area of the PMMA/CVD-hBN assembly from the etchant solution.
6. While the PMMA/CVD-hBN is floating on DI water, we transfer it on to a desired substrate (either a stack on a SiO₂/Si wafer for device preparation or another hBN/Cu/hBN for preparing bi or tri-layers of CVD-hBN) by submerging it into the water underneath the floating PMMA/CVD-hBN structure.

7. In Chapter 7, we prepare a two-layer-CVD-hBN stack. For this, above steps are repeated to prepare the two-layer-CVD-hBN and subsequently transfer on top of an already prepared graphene/hBN stack on a SiO₂/Si substrate.
8. The final substrate with the transferred CVD-hBN layer is baked on a hotplate at 180 °C for 2 minutes to remove the remaining water. This will relax PMMA and increase the adhesion of CVD-hBN to substrate.
9. Since the PMMA on top is too thick for lithography, eventually, it is dissolved in acetone at 40 °C for 10 minutes.
10. The resulting stack is annealed again in an Ar/H₂ atmosphere at 350 °C for 12 hours to remove any PMMA residues leftover on the topmost layer.

The PMMA assisted method allows for an easy transfer of a continuous as-grown CVD-hBN onto any substrate. However, due to the nature of the wet-transfer method, the resulting electronic quality of the graphene devices can degrade. The residues of PMMA could dope the graphene. During the wet-transfer, graphene comes in a contact with DI-water and also the organic residues may get trapped at the graphene/CVD-hBN interface. The resulting water bubbles at the graphene/hBN interface may crack the CVD-hBN during the annealing on a hot plate step. Furthermore, un-etched copper residues may contaminate graphene. This process can be the most time consuming of all the steps involved in preparation of a graphene spin valve device. The importance of these issues will be discussed in the Chapter 7. In order to overcome these problems, one can adopt the recently developed dry-transfer technique where the CVD material can be directly picked up using a thick-hBN flake and transferred onto a desired substrate.

4.2.4 Lithography for electrodes deposition

The cleaned device from the previous step is ready for the lithography and ferromagnetic electrode position. The electrodes are patterned via the electron beam lithography on the PMMA coated hBN/Gr/hBN stack. The lithography and the subsequent electrode deposition procedure is same for all the samples prepared in this thesis.

1. The cleaned device is baked on a hot plate at 180 °C for 90 s at atmospheric pressure to remove any moisture on the device.
2. An e-beam resist PMMA (950K, 4 wt.%) is spincoated on the sample at 4000 rpm followed by repeating the annealing step to remove any solvent in the resist.
3. A small scratch is made as a reference to design reference markers for EBL. The design is made using the RAITH software.

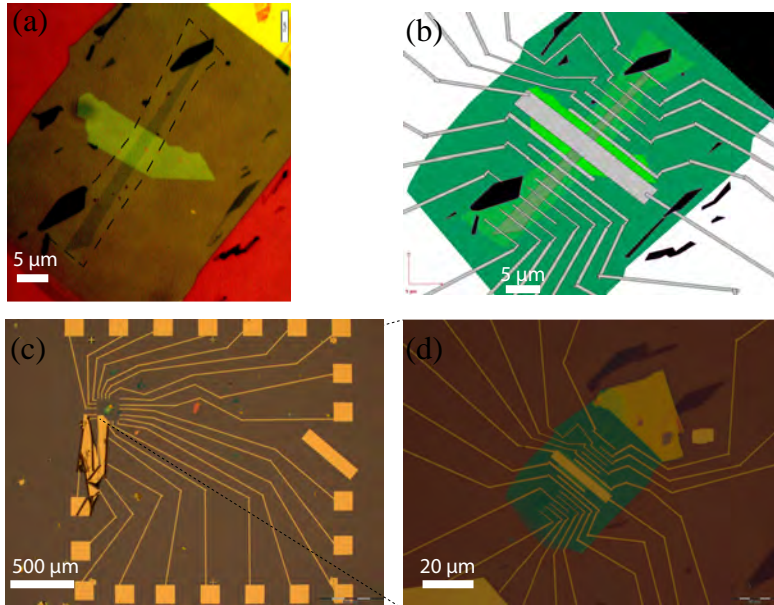


Figure 4.2: Graphene spin valve device during the lithography steps. (a) Optical image of a fully hBN encapsulated graphene stack. All the flakes are mechanically exfoliated. Thin layer of encapsulating hBN tunnel barrier (3 layers ≈ 1.2 nm) is not visible and is outlined with black dashed lines. A thick top hBN is additionally used which can be used as a top gate dielectric. (b) Contacts design for EBL made using RAITH software. (c) Optical image of the device after lift-off. A small region of under lift-off area close to the stack is probably due to overexposure of PMMA during EBL. (d) A close up of the stack with electrodes.

4. The device is loaded into an EBL setup and the small alignment markers were exposed using an electron beam (e-beam) at 10 keV and with $150 \mu\text{Ccm}^{-2}$ dose.
5. The markers were developed in MIBK:IPA (1:3) solution which selectively removes the PMMA exposed to the e-beam.
6. Using these markers as a reference, a contact design was made for graphene using RAITH software. In order to get different switching coercive fields for different ferromagnetic electrodes, no two contacts were designed with equal widths. The contacts are also designed in a rectangular shape to avoid the domain coupling with the regions far from graphene.
7. The device is loaded again into the EBL setup and the contacts were exposed with the same beam parameters as before.
8. The patterned sample is developed again but this time to remove the exposed PMMA for contacts. The resulting device is imaged with the an optical micro-

scope to check the accuracy of positioning of the patterned contacts on graphene. In case of misplaced contacts, PMMA will be dissolved in acetone at 50 °C, followed by annealing in Ar/H₂ at 350 °C and repeat the lithography steps from the beginning.

9. Now the sample is loaded in electron beam evaporation chamber (Temescal 2000) for the deposition of ferromagnetic cobalt of 60 nm thick on top of the hBN tunnel barrier. Vacuum pressure is maintained at 1×10^{-7} mbar during the deposition. To prevent the oxidation of the cobalt electrodes, they are covered with a 3 nm thick aluminum layer.
10. The evaporated material on top of the unexposed polymer is removed via the lift-off process in hot acetone at 50 °C, leaving only the contacts in the desired area. Usually it takes 5-10 minutes. This is followed by rinsing the sample with IPA and blow dry with N₂ gas. The device is then inspected with the optical microscope again for identifying any anomaly in the deposited contacts.
11. The substrate is then carefully glued on top of a 24-pin chip carrier using a silver paste while aligning the contacts orientation along the edge of the chip carrier. This is to make sure that the magnetic field in our measurement setup is along the longitudinal direction of contacts.
12. The large FM bond pads of the device and the back gate electrode, *p* + + Si, are connected to the pins of the chip carrier by AlSi (Al 99% and Si 1%) wires which provide the electrical contact to the external electronics.
13. The chip carrier with the sample is then placed in a sample holder and together with it is loaded in a vacuum-can and is pumped down to pressures below 1×10^{-5} mbar and ready to be electrically characterized with a measurement setup.

4.3 Measurement setup

The measurement setup consists of a switch box, lock-ins, Keithleys, an in-house made IV-measurement box, an electromagnet, a power supplier for the magnet, and a computer with the Labview software to remotely control the aforementioned instruments.

The chip carrier is clamped on a sample holder, which is electrically connected to the source/measurement equipment. A representative schematic of the measurement setup is shown in Fig. 4.3(a). The sample holder is inserted into a vacuum chamber in a liquid Helium flow cryostat that is fixed in between the poles of the electromagnet, which can apply a magnetic field up to 1.2 T depending on the separation between the

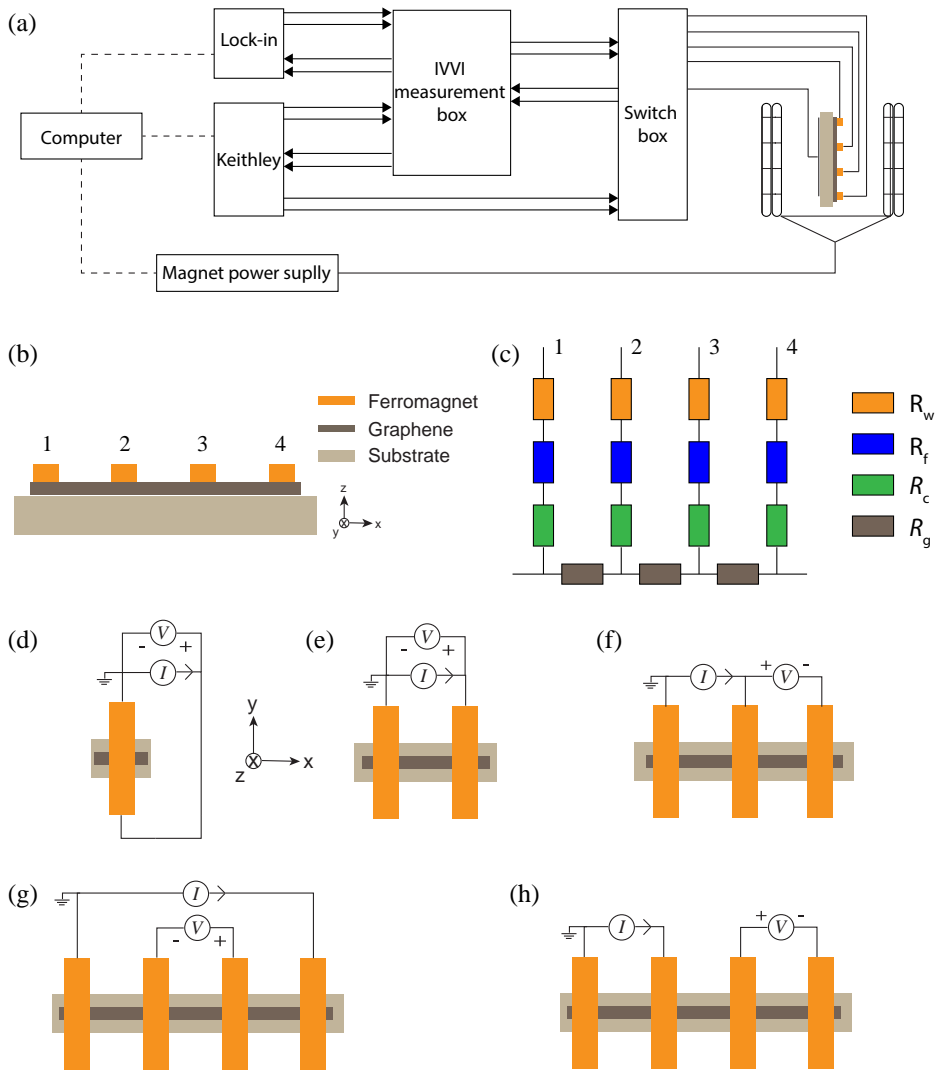


Figure 4.3: (a) Schematic of a measurement setup. (b) Schematic side view of a device with four contacts. (c) Schematic of an equivalent circuit for the device shown in (b). (d)-(h) show schematic top view of measurement geometries with electrical connections. (d) Two-terminal geometry for verifying electrical connections of the setup. (e) Two-terminal geometry for checking connection between the contacts of the device as well as for two-terminal spin valve and Hanle measurements. (f) Three-terminal geometry for contact characterization as well as for Hanle measurement. (g) Four-terminal local geometry for graphene characterization. (h) Four-terminal nonlocal geometry for spin valve and Hanle measurements.

poles. The electromagnet can be rotated around the cryostat so that the magnetic field direction can be changed with respect to a fixed orientation of the sample inside the vacuum can. We try to minimize the time between the post electrode-deposition step and loading the sample in the vacuum chamber in order to reduce the oxidation of cobalt electrodes in air. The vacuum chamber is then pumped down to a pressure less than 10^{-6} mbar in order to protect the sample from the environmental contamination that can influence the transport properties of graphene.

All the contacts of the sample are electrically connected to a switch box. The switch box is connected to the lock-ins or Keithleys via BNC (after its Bayonet mount locking mechanism and its inventors, Neill Paul and Concelman Carl) and/or LEMO (after the founder of LEMO company, Léon Mouttet) cables. The switch box is equipped with three-way switches that act as interconnects between the sample contacts and the common ground or float or connection with the source/measurement equipment. The lock-ins can source a sinusoidal voltage signal v_{out} with RMS amplitude between 0 and 5 V at a specified frequency, typically below 20 Hz, and can measure the voltage signals v_{in} . IV-measurement box consists of a current source and voltage pre-amplifiers. The current source is controlled by an external voltage. In case of sourcing an AC current, the external voltage input is from the lock-in while in case of sourcing the DC current, the voltage input is from the Keithley. The conversion factor of the current source ranges from 1 pA/V to 100 mA/V. Using our home-made IV-measurement box, we can also source both the AC and DC currents simultaneously by giving the voltage input from both lock-in and Keithley to the IV-measurement box. This feature has been used for the bias dependent differential spin signal measurements in Chapters 6 and 7. The resulting current signal is sourced to the device via the switch box and the response voltage signal is passed to the pre-amplifier, again, via switch box.

The voltage pre-amplifier of the IV-measurement box amplifies the signal received from the sample. The pre-amplified signal is measured via the lock-ins for measuring a differential signal or Keithleys for measuring a DC signal. The amplification factor of the pre-amplifiers ranges from 10^0 to 10^5 . When both AC and DC current sources are simultaneously applied for spin injection measurements, one can measure the differential spin signal via the lock-in and the DC signal via the Keithley. The measured signals from lock-ins and Keithleys can be read out using the Labview program on a computer.

4.4 Electrical Characterization

For most of the electrical measurements performed in this thesis, we employed the low-frequency lock-in detection technique for measuring the differential signals. The lock-in technique allows to measure the signals of a small magnitude at zero-bias

at low frequencies (long measurement time). We also utilized the DC detection technique for finite-bias measurements and for backgate tuning using DC voltmeters (Keithleys). A pure DC method allows to measure the signals on a short time scale, however, usually resulting in a poor signal to noise ratio compared to the lock-in technique. Therefore, typically, a large magnitude of current, i.e., large-bias is required for the DC detection method. In order to detect low-bias dependent signals, we use a DC current source along with an AC current, and detect the differential signal using the lock-in.

A complete electrical characterization of a graphene device requires to use multiple measurement geometries, each with its own purpose. For a clear understanding of the measurements, an equivalent circuit diagrams of electrical connections and the device are shown in Fig. 4.3 which includes different types of resistors; graphene resistance R_g , contact resistance R_c that is the sum of the resistances of graphene/tunnel barrier and the tunnel barrier/electrode interfaces, wire resistance R_w that includes the cable connectors and the lithographically defined metallic electrodes, and filter resistance R_f inside the switch box.

4.4.1 Charge transport measurements

Two terminal check-1: Right after loading the sample in the measurement setup, we first measure the voltage across a short circuit in order to check the electrical connectivity of the setup. Here we source a current across a running contact and measure a voltage across the same terminals[Fig. 4.3(d)]. This is a two-terminal measurement however, graphene does not come into the circuit. We know that all the filters in the switch box are same. Assuming R_w of all contacts is same, we can determine R_w . Typical value of $R_w \approx 100\text{-}200 \Omega$.

Two terminal check-2: We then check if all the contacts of the device are working properly using the two-terminal measurement geometry. Here a current is passed between two contacts and the voltage is detected across the same pair of contacts[Fig. 4.3(e)]. The total measured resistance will be $R_{f,1} + R_{w,1} + R_{c,1} + R_g + R_{c,2} + R_{w,2} + R_{f,2}$. Since R_c and R_g vary for different combination of two terminals, this geometry does not give a clear information about the nature of the contacts and the graphene channel, and only used for verifying the functioning of contacts of the contacts. Following two measurement geometries are used for characterization of contacts and graphene channel separately.

Three terminal measurement: For the characterization of the contacts, a three-terminal geometry is used. Here, a current source and voltage detector are connected to only one terminal[Fig. 4.3(f)]. The total measured resistance will be $R_f + R_w + R_c$. Since we know R_w from the first check and that R_f is constant, we can determine R_c from the three-terminal measurements. Generally, two types of three-terminal measurements are performed for the electrical characterization of the contacts. One

is the I-V characterization where a DC current is sourced with the IV-measurement box as explained before and a DC voltage is measured with a Keithley. The other one is the differential- R_c Vs I(or V) measurements, where a DC current along with a fixed magnitude of the AC current is sourced with the IV-measurement box and the differential signal is measured with the lock-in and the DC voltage is measured with the Keithley.

Four terminal measurement: Local For the characterization of the charge transport in graphene channel, four-terminal local geometry is used. Here, a current is sourced between two contacts and a voltage is measured across two contacts in between[Fig. 4.3(g)]. The total measured resistance, R_g , is only the flake resistance. In order to measure the charge transport properties of the graphene channel, we apply a backgate voltage using a Keithley to the gate electrode while measuring R_g .

4.4.2 Spin transport measurements

Four terminal non-local measurement: Spin valve and Hanle signals For spin transport characterization, we use a four-terminal non-local geometry. Here, a current is passed between two terminals and a voltage drop is measured between the two terminals which are located outside the charge current path[Fig. 4.3(h)]. Since there is no charge current flow in the voltage detection circuit, the measured resistance has no contribution from the charge transport. The ferromagnetic electrodes are spin selective and the detection voltage is sensitive to the spin accumulation underneath the detectors that is diffused from the injector contacts. Therefore the measured non-local voltage is non zero. The non-local spin accumulation is detected in two types of measurements: i) Spin valve measurements with an in-plane magnetic field applied along the easy axes of the magnetization of ferromagnetic electrodes, and ii) Hanle spin precession measurements with the magnetic field applied perpendicular to the device plane. See Chapter 2 for principles behind these measurements.

Two terminal local measurements: Spin valve and Hanle signals The two-terminal geometry is much simpler than the four-terminal nonlocal geometry for characterizing the spin transport. Here, both the current injection and voltage detection probes are connected across the same two terminals[Fig. 4.3(e)]. The measured signal is a result of the contact resistances which includes the contribution from the injected spin accumulation underneath each contact, the channel resistance, and the diffused spin accumulation from one contact to the other. However, due to a very small magnitude of the commonly observed spin signals compared to the accompanied charge contribution signals, the two-terminal geometry is rarely used for spin transport studies. Besides, the interpretation of the measurements is often difficult due to spurious magnetoresistance signals that could mimic the spin signals. Similar to the nonlocal geometry, one can detect the spin accumulation in the spin valve and Hanle spin precession measurements in the two-terminal geometry. The

details are provided in Chapter 2 for principle behind these measurements. See Chapter 6 for a large magnitude of spin signals measured in the two-terminal spin valve measurement geometry and Chapter 8 for two-terminal Hanle spin precession measurements.

References

- [1] Lu, X. *et al.* Tailoring graphite with the goal of achieving single sheets. *Nanotechnology* **10**, 269 (1999).
- [2] Zhang, Y. *et al.* Fabrication and electric-field-dependent transport measurements of mesoscopic graphite devices. *Appl. Phys. Lett.* **86**, 073104 (2005).
- [3] Novoselov, K. S. *et al.* Electric field effect in atomically thin carbon films. *Science* **306**, 666–669 (2004).
- [4] Stauber, T., Peres, N. M. R. & Geim, A. K. Optical conductivity of graphene in the visible region of the spectrum. *Phys. Rev. B* **78**, 085432 (2008).
- [5] Nair, R. R. *et al.* Fine structure constant defines visual transparency of graphene. *Science* **320**, 1308–1308 (2008).
- [6] Blake, P. *et al.* Making graphene visible. *Appl. Phys. Lett.* **91**, 063124 (2007).
- [7] Novoselov, K. S. *et al.* Two-dimensional atomic crystals. *Proceedings of the National Academy of Sciences of the United States of America* **102**, 10451–10453 (2005).
- [8] Pacilè, D. *et al.* The two-dimensional phase of boron nitride: Few-atomic-layer sheets and suspended membranes. *Appl. Phys. Lett.* **92**, 133107 (2008).
- [9] Lee, C. *et al.* Frictional characteristics of atomically thin sheets. *Science* **328**, 76–80 (2010).
- [10] Gorbachev, R. V. *et al.* Hunting for monolayer boron nitride: Optical and Raman signatures. *Small* **7**, 465–468 (2011).
- [11] Ferrari, A. C. *et al.* Raman spectrum of graphene and graphene layers. *Phys. Rev. Lett.* **97**, 187401 (2006).
- [12] Dean, C. R. *et al.* Boron nitride substrates for high-quality graphene electronics. *Nature Nano.* **5**, 722–726 (2010).
- [13] Zomer, P. J. *et al.* Fast pick up technique for high quality heterostructures of bilayer graphene and hexagonal boron nitride. *Appl. Phys. Lett.* **105**, 013101 (2014).
- [14] Lee, Y. *et al.* Wafer-scale synthesis and transfer of graphene films. *Nano Lett.* **10**, 490–493 (2010).
- [15] Song, X. *et al.* Chemical vapor deposition growth of large-scale hexagonal boron nitride with controllable orientation. *Nano Research* **8**, 3164–3176 (2015).

